AIAA JOURNAL
Vol. 33, No. 11, November 1995

Effects of Mean Flow Three Dimensionality on Turbulent Boundary-Layer Structure

John K. Eaton*
Stanford University, Stanford, California 94305

Several experimental studies examining the near-wall structure of three-dimensional turbulent boundary layers are reviewed. The reduction of the Reynolds shear stress by the mean flow three dimensionality is a common feature of all of these flows. The near-wall region ($y^+ < 100$) is found to be dominated by quasistreamwise vortices and low- and high-speed streaks similar to two-dimensional boundary layers. However, the development of the vortices and their production of shear stress is modified by the presence of mean flow skewing across the near-wall zone. The implications of these findings are discussed.

I. Introduction

TURBULENT boundary layers have been the focus of research for many years because they occur so commonly in engineering devices. Most of the detailed research has been conducted in flows where the mean flow is two dimensional even though most practical boundary layers have a three-dimensional mean flow. Examples of flows that produce three-dimensional turbulent boundary layers are the endwalls of curved ducts, swept aircraft wings, flows around surface-mounted obstacles, and rotating disks. For many years it was assumed that mean flow three dimensionality would have little effect on the turbulence, but as we will see below, this is not the case.

In recent years there has been considerably more effort to understand how mean flow three dimensionality affects the turbulence properties and to provide data sets for computational fluid dynamics (CFD) comparisons. Johnston and Flack[1] have reviewed recent three-dimensional turbulent boundary layers studies focusing on the mean velocity development and single point turbulence statistics with a brief discussion of the turbulence structure. There is now a large enough set of experiments available that a reasonably coherent description of three-dimensional effects on turbulence statistics is emerging.

To discuss our current understanding we consider a simple flow in which a spanwise pressure gradient is imposed on an initially two-dimensional boundary layer. The flow turns in response to the pressure gradient with the flow near the wall turning through a greater angle than the freestream, resulting in a skewing across the boundary layer. We choose a coordinate system in which x is aligned with the local freestream direction, y is normal to the wall, and z is selected to complete a right-handed system. Typical mean velocity profiles for u and w are shown in Fig. 1. The important point to note is that there is distributed longitudinal vorticity (ω_x) throughout the boundary layer with the vorticity levels being quite low in the outer layer and much higher near the wall. The important Reynolds stress components determining the development of the boundary layer are $\overline{u'v'}$ and $\overline{v'w'}$. These components form a vector parallel to the wall that is commonly called the shear stress vector. One important effect of three dimensionality is that the shear stress vector is not aligned with the velocity gradient vector that has components $\partial U/\partial Y$ and $\partial W/\partial y$. In flows that are rapidly turned, the misalignment can be very large. A more important effect is that the magnitude of the shear stress vector is reduced relative to two-dimensional boundary layers. Johnston and Flack compiled data from 10 different three-dimensional turbulent boundary-layer experiments and plotted $a_1 = \tau_t/q^2$ where τ_t is the magnitude of the shear stress vector and q^2 is twice the turbulent kinetic energy. Every experiment shows that the value of a_1 is suppressed substantially below the value of 0.15 commonly found in two-dimensional boundary layers. The only experiments available indicate that the vertical transport of thermal energy also is suppressed by mean flow three dimensionality (Abrahamson and Eaton[2]).

Although the reduction in shear stress is well established, the causes of this reduction are not understood. Clearly there must be some distortion of the dominant turbulence structure by the three dimensionality. However, the details of this distortion have only been addressed very recently. Bradshaw and Pontikos[3] hypothesized that large eddies are overturned by the crossflow rotating them out of their optimal orientation for producing shear stress. This implies that the three dimensionality would only reduce the shear stresses during a transition from two-dimensional to three-dimensional flow. However, three-dimensional turbulent boundary layers that have three dimensionality imposed from their inception (e.g., rotating disk flow) show a similar reduction in shear stress. Anderson and Eaton[4] felt that the reduction in shear stress must be related to the interaction of longitudinal vortex structures near the wall with the layer of distributed longitudinal vorticity associated with the crossflow. The peak in turbulent shear stress production occurs around $y^+ = 20$ and two-dimensional turbulent boundary layer research has shown that longitudinal vortices are the dominant structure in this region (see the review of Robinson[5]). The peak in the crossflow velocity profile usually occurs between about y^+ of 50 and 100 meaning that the longitudinal vortices are embedded in the layer of high longitudinal vorticity. Anderson and Eaton hypothesized that longitudinal vortices of sign opposite the distributed vorticity would be destroyed, leaving only a single sign of vortices to produce shear stress.

The hypotheses of Bradshaw and Pontikos and Anderson and Eaton were based on intuition and single-point measurements. By the late 1980s there had been no direct structural experiments using flow visualization or multipoint measurement techniques. This situation has changed with a number of groups making a concerted effort to understand the observed changes in the Reynolds stresses. This paper describes a series of experiments conducted in the author's laboratory specifically to investigate distortion of near-wall

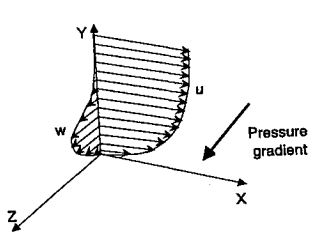

Fig. 1 Typical velocity profile for a pressure-driven three-dimensional turbulent boundary layer (from Ref. 10).

Presented as Paper 94-2225 at the AIAA 25th Fluid Dynamics Conference, Colorado Springs, CO, June 20–23, 1994; received June 23, 1994; revision received March 31, 1995; accepted for publication April 3, 1995.

*Professor, Department of Mechanical Engineering. Senior Member AIAA.

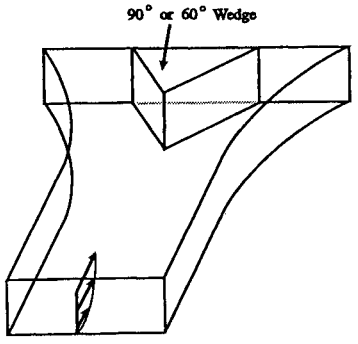

Fig. 2 Flow studied by Anderson and Eaton (from Ref. 9).

turbulence structure. The purpose here is to show how a consistent picture of the structural modification has emerged. Brief mention will be made of related work in other laboratories, but this paper is not intended to be a comprehensive review.

II. Structural Studies

A. Flow Approaching a Wedge

The first direct examination of the structural features of a three-dimensional turbulent boundary layer was reported by Anderson and Eaton,[4] who studied an initially two-dimensional boundary layer that was skewed by the spanwise pressure gradient ahead of an upstream facing wedge. The test section geometry is shown in Fig. 2. The main experiment comprised single-point measurements of the mean velocity and turbulence stresses, but a low-Reynolds-number analog of the experiment was built in a smoke tunnel to examine the near-wall structure. Smoke was seeped into the sublayer through a spanwise slot and was concentrated into the sublayer streaks. Illumination was by a thick sheet of light parallel to the wall. Photographs were taken in the upstream two-dimensional turbulent boundary layer and in the highly skewed boundary layer upstream of the wedge. The streak spacing appeared to be roughly the same in the two regions of the flow. However, the streaks appeared more stable in the three-dimensional region, suggesting that bursting occurs less frequently in the skewed flow. No detailed analysis was done of the flow visualization, but the qualitative results bolstered our opinion that the mean flow three dimensionality was in some way interfering with longitudinal vortex structures near the wall.

B. Experiments with Embedded Vortices

Shizawa and Eaton[6,7] examined the development of longitudinal vortices in a three-dimensional turbulent boundary layer using a vortex generator to embed a vortex in the wedge flow boundary layer. The vortex generator was a small half delta wing mounted on the wall with a height approximately equal to the boundary-layer thickness. Therefore, the vortex had a diameter of the same order as the boundary-layer thickness as opposed to the much smaller vortices that occur naturally in the near-wall region of a boundary layer. Despite that difference, we believe that the results lend insight into to the natural development of three-dimensional turbulent boundary layers.

Two different cases were examined with the parameter being the sign of the vortex rotation. A case 1 vortex is one whose circulation is in the opposite direction of ω_x associated with the crossflow profile near the wall (see Fig. 3). Therefore, the vortex-induced velocity near the wall is in the same direction as the crossflow. A case 2 vortex has the opposite sense of rotation.

The vortices were generated in the upstream two-dimensional section, and their downstream development was mapped by measuring all components of the mean velocity vector and the Reynolds stress tensor at five downstream planes. The initial vortex position was selected for each case so that the vortex center passed through one of Anderson and Eaton's primary measurement stations midway through the three-dimensional test section. Measurements were acquired using a five-hole probe for the mean velocity, and a rotatable x-array hotwire anemometer supplying redundant mean velocity measurements and all components of the Reynolds stress tensor.

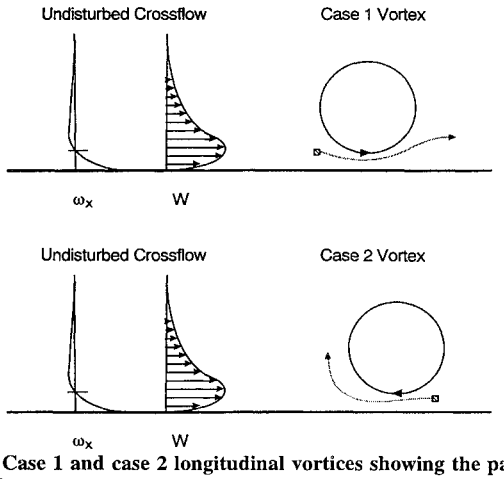

Fig. 3 Case 1 and case 2 longitudinal vortices showing the path of a typical fluid particle moving under the vortex.

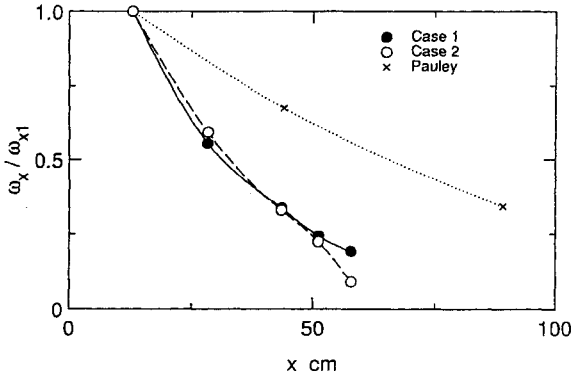

Fig. 4 Peak vorticity development for a longitudinal vortices embedded in two- and three-dimensional boundary layers (from Ref. 6).

The measurement points within the planes were closely spaced allowing direct differentiation to obtain ω_x.

The most important results in the present context are the mean velocity data. These data indicate that the vortex dies out much more quickly in a three-dimensional turbulent boundary layer than in an equivalent two-dimensional flow. Figure 4 shows the axial variation of the peak value of ω_x in the vortex core. These data are compared with the earlier study of Pauley and Eaton[8] for a vortex embedded in a two-dimensional turbulent boundary layer. Shizawa and Eaton concluded that the gradient of the crossflow velocity stretches and tilts the vortex into an orientation that is subject to stronger vorticity diffusion. This suggests that mean flow three dimensionality might act to reduce the strength of the naturally occurring longitudinal vortices. However, the change in flow direction across the natural vortices is much smaller than for the large embedded vortices. The more important results here are the axial mean velocity measurements shown in Figs. 5 and 6. These figures show important differences between the two cases. A case 1 vortex produces the usual distortion at the upstream stations, namely, a thinning of the boundary layer on the downwash side of the vortex and an increase in the thickness on the upwash side. The buildup of low-speed fluid on the upwash side corresponds to the formation of low-speed streaks by naturally formed longitudinal vortices in an unperturbed boundary layer. The perturbation dies out very quickly in the three-dimensional flow, leaving only a minor ripple in the axial velocity contours at the most downstream section. Contrast this to the case 2 vortex that shows a stronger perturbation that continues to grow up to the final measurement station. To understand this we examine the path of a fluid particle that is swept under the vortex as illustrated in Fig. 3. In case 1, the particle moves under the vortex and then begins to move upward on the upwash (right) side of the vortex. However, the crossflow continues to carry the fluid particle to the right, away from the upwash so that its vertical motion ceases. In case 2, the particle is again swept under the vortex, only this time moving to

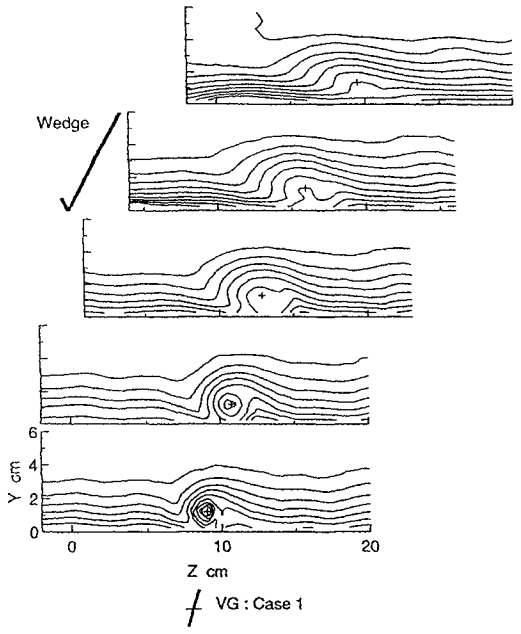

Fig. 5 Axial mean velocity for a case 1 vortex. Outer contour level, $U/U_e = 0.99$. Contour interval, $U/U_e = 0.05$ (from Ref. 7).

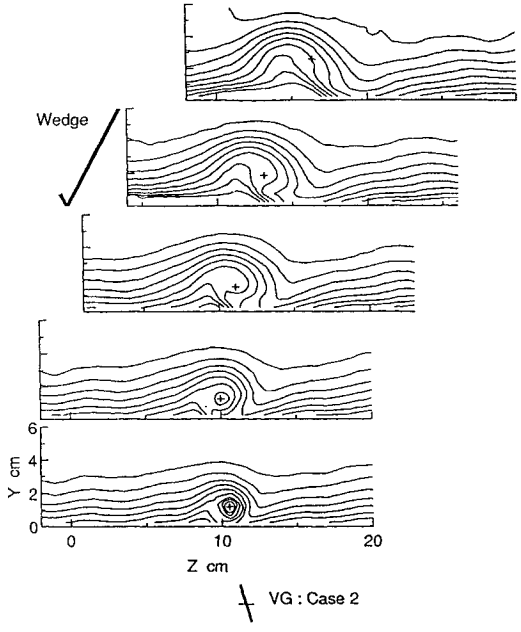

Fig. 6 Axial mean velocity for a case 2 vortex. Contour levels as in Fig. 5 (from Ref. 7).

the left. In this case, the crossflow opposes its motion, holding the particle in the upwash side of the vortex. The particle is swept far from the wall, producing the effects illustrated in Fig. 6.

The relevance of these measurements to a natural three-dimensional turbulent boundary layer is not well established. However, the data suggest that the original hypothesis of Anderson and Eaton that a crossflow would destroy one sign of longitudinal vortex was incorrect. It seems likely that vortices of either sign would still be present in the boundary layer. Instead, the crossflow inhibits the ability of case 1 vortices to produce low-speed streaks. Also, by suppressing crossflow separation, the crossflow should reduce or eliminate the ability of the case 1 vortices to produce ejections of low-momentum fluid away from the wall. Since these ejections are one of the two (the other being sweeps) dominant producers of shear stress, this would result in a substantial reduction in the shear stress. The reduction in the strength of some of the streaks may also lead to a decrease in longitudinal vortex formation.

C. Experiments on a Rotating Disk

Further structural studies were performed on the flow over a large disk rotating in a quiescent environment. This flow was selected for its geometrical simplicity. In this case, the crossflow is produced by centrifugal force rather than a pressure gradient, but the effects are quite similar. The mean profiles appear much like those in Fig. 1 when examined in a coordinate system rotating with the disk.

Our first experiment on this flow was performed by Littell and Eaton[9,10] using a 1-m-diam disk rotating in air at speeds up to 1500 rpm. Single-point turbulence statistics were obtained for momentum thickness Reynolds numbers up to 6×10^3 and indicated that shear stress was reduced in this flow much like in the pressure-driven three-dimensional turbulent boundary layers. Unlike the other experiments, there was a strong suppression of turbulent activity in the wake region of the flow leading to a mean velocity profile with virtually no wake component. Similar results were found by Senoo and Nishi,[11] who investigated an endwall flow turned through a large angle. Littell and Eaton concluded that the absence of a wake was a characteristic of an equilibrium three-dimensional turbulent boundary layer.

The structure was examined in the disk flow using two-point correlations measured by a pair of crosswires. The crosswires were mounted on a common stem that allowed a variable separation between the probe tips. The probes were aligned with the mean flow streamlines (in the laboratory reference frame) and the separation was normal to the streamlines. Single-point statistics were measured by each probe separately to check for interference, and excellent agreement was obtained, indicating that the wake of the inner probe passed outside of the outer probe. Correlation measurements were acquired at one height ($y = 1.641$ mm) for two different Reynolds numbers, $Re_\theta = 2.66 \times 10^3$ and 4.97×10^3. At these Reynolds numbers the probe height corresponded to 110 and 210 wall units, respectively.

Extensive documentation of the two-point correlations is provided in the background papers[10,11] with only the most pertinent results presented here. Figure 7 shows the correlation coefficient R_{12} where the nomenclature means that the first probe measures the longitudinal (tangential) velocity component and the second probe measures the wall-normal component. Positive separation means that the second probe is radially outboard. Four sets of measurements are reported showing the lack of sensitivity to Reynolds number or probe orientation. The important feature on this plot is the strong asymmetry about the zero separation axis. This quantity must be symmetric in a two-dimensional turbulent boundary layer.

A greater understanding of the flow was obtained by conditionally averaging the velocity measurements from one probe based on the velocity measured at the other probe. In other words we asked the question: What is the velocity field surrounding a given triggering event? Figure 8a shows the conditionally averaged vertical velocity fluctuation surrounding a strong vertical velocity fluctuation at the trigger point. Strong in this case is defined as greater than 1.4 times the rms value. The plot is symmetric about the zero separation line with a significant negative dip on either side of the central maximum. We interpret these results in terms of the two-dimensional boundary layer structure model described by Robinson.[5] In that model, strong vertical velocity fluctuations near the wall are produced by longitudinal vortices. The upwash side of a longitudinal

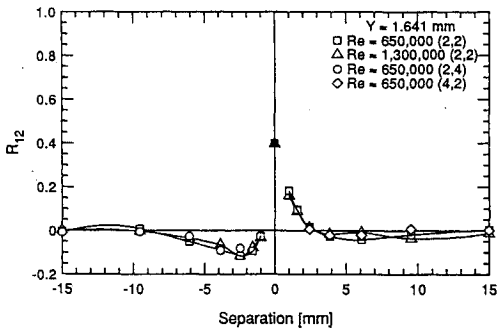

Fig. 7 Correlation coefficient R_{12} for radial probe separation in the disk flow (from Ref. 10).

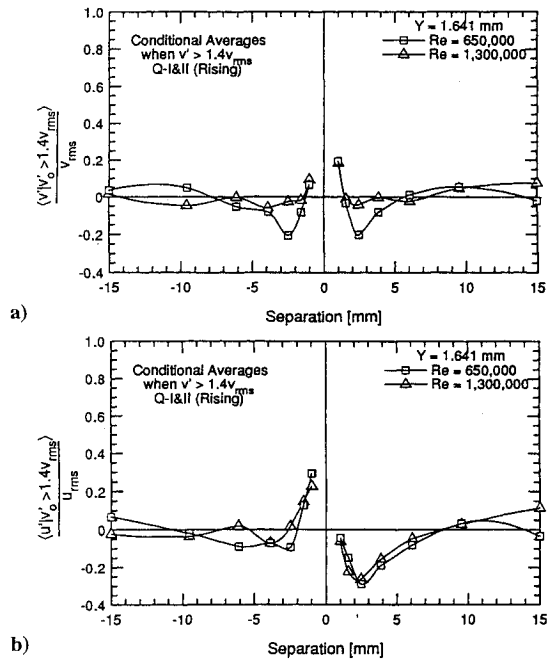

Fig. 8 a) Average vertical velocity and b) average streamwise velocity around a strong vertical velocity fluctuation.

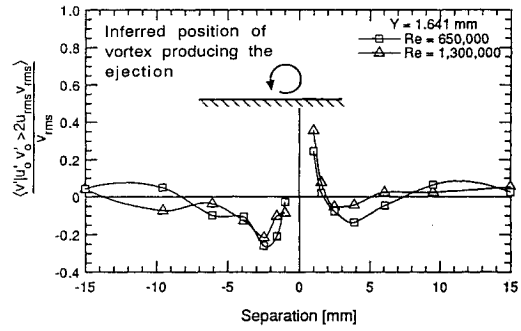

Fig. 9 Average vertical velocity around an injection event.

vortex produces the positive vertical velocity, and there should be negative vertical velocity on the other side of the vortex. The symmetry of Fig. 8a implies that vertical velocity fluctuations are equally likely to be produced by either case 1 or case 2 vortices. Figure 8b shows the average streamwise velocity fluctuation surrounding a strong vertical velocity fluctuation. The plot is asymmetric, indicating that the two signs of vortices produce unequal distortions of the streamwise velocity. This is the same effect as observed by Shizawa and Eaton[7] for much larger vortices.

The most revealing plot is Fig. 9, which shows the vertical velocity conditioned on the occurrence of an ejection at the trigger point. An ejection is defined as positive vertical and streamwise velocity fluctuations producing an instantaneous shear stress value greater than $2\sqrt{(\bar{u}'^2)}\sqrt{(\bar{v}'^2)}$. (In the rotating disk flow the highest streamwise velocities are adjacent to the disk so that positive shear stress corresponds to positive $u'v'$.) Here we see a strong asymmetry; there is a significant negative dip on the inboard side, whereas the velocity decays nearly monotonically to zero on the outboard side. This indicates that most ejections are produced by vortices that are inboard of the ejection. Those vortices produce the inboard dip as indicated by the sketch in the corner of Fig. 9. The vortex sketched in Fig. 9 is a case 1 vortex using our earlier definitions. The two-point correlation measurements thus indicate that ejections produced by case 1 vortices are stronger than case 2 vortices. We took this to mean that ejections produced by case 2 vortices are weakened in three-dimensional turbulent boundary layers rather than case 1 ejections are strengthened. This conclusion was reached because the overall level of shear stress is reduced in three-dimensional turbulent boundary layers. Additional conditioned measurements that are not shown here indicate that sweep events are most often produced by case 2 vortex structures. Again we interpreted that as indicating that sweeps produced by case 1 vortices are weakened. Putting the entire picture together, we concluded that the reduction in shear stress in three-dimensional turbulent boundary layers was due to a reduction of the effectiveness of longitudinal vortices at producing ejections and sweeps. In a two-dimensional turbulent boundary layer a longitudinal vortex produces both ejections and sweeps, but in the disk boundary layer, case 2 vortices are inhibited from producing strong ejections and case 1 vortices are inhibited from producing strong sweeps. This finding contradicts the previous hypothesis that was based on Shizawa and Eaton's work. This is probably due to the large differences in the size and strength between the naturally occurring and artificially generated vortices.

Detailed interpretation of two-point correlation data is risky because a basic structure must be assumed to interpret the results. Chiang and Eaton[12] conducted a disk flow experiment in water in hopes of using flow visualization to corroborate or refine the earlier conclusions. A 1-m-diam disk was again used, but in this case there was a 16.5-cm-diam hub that rotated with the disk. Single-point measurements were acquired using an LDA system at a radius of 40 cm for Re_θ ranging from 3.1×10^3 to 5.3×10^3. These data showed excellent agreement with the results of Littell and Eaton. Visualization was performed at a lower Reynolds number ($Re_\theta = 1.9 \times 10^3$) to provide the slowest flow speed and thickest sublayer possible while still retaining a developed turbulent boundary layer. A hydrogen bubble wire was placed along a radial line, parallel to the disk surface at a height of $y^+ = 40$. The bubbles were illuminated by a laser sheet normal to the surface along a radial line 1 cm downstream of the bubble wire. The near-wall structures were convected through the sheet carried by the rotating disk. A high-speed 16-mm movie camera was used to record the visualization at a rate of 1000 frames/s. The camera zoom lens and a second lens were used to achieve high magnification since the typical streak spacing in the flow was on the order of 2 mm. Because of the small scale of the flow, the only events that could be successfully visualized were ejections that carry clusters of bubbles far from the wall.

Using frame-by-frame examination of the movies, we identified a total of 220 ejection events. Typically, a cluster of bubbles was lifted rapidly away from the wall and then curled to one side or the other. If the curling was toward the disk center, we interpreted the event as being induced by a case 1 vortex and vice versa. The events were roughly evenly distributed between cases 1 and 2 (48–52%), but the apparent strength of the ejection and the detailed motion of the bubble cluster were different for the two cases. The maximum height of the ejection for case 1 events averaged 100 wall units, whereas the average was only 80 for the case 2 events. This observation led to a further refinement of Littell and Eaton's conclusions. We see that case 1 and 2 vortices are equally likely to produce ejection events but that the ejections induced by case 2 vortices are substantially weaker. This can account for the asymmetry observed in the two-point correlation data.

Detailed examination of the ejection events led to a better understanding of how the crossflow reduces the strength of ejections produced by case 2 vortices. This mechanism is illustrated in Fig. 10. The peak crossflow velocity has been shown at a y^+ value of approximately 30 that is appropriate to the low Reynolds number of the visualization experiment. The longitudinal vortex is centered at a height of about 30 wall units. In the boundary layer there are a range of vortex sizes and positions, but the vortex shown would be midway in the range of scales typically encountered (see Robinson[5]). There are two paths shown for a fluid particle beginning near the wall. The

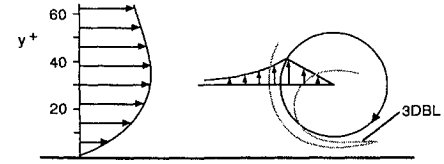

Fig. 10 Sketch of possible mechanism explaining reduced strength of ejections produced by case 2 vortices.

first path is the one that would occur in the absence of the crossflow. The particle is swept under the vortex and then lifted away from the wall, eventually curling over the top of the vortex. With the crossflow present, the particle follows the path labeled three-dimensional boundary layer. The fluid element again is swept under the vortex, but as it begins to lift away from the wall, the crossflow pushes it back towards the center of the vortex. The particle moves into the region of low vertical velocity near the vortex center and begins to move horizontally. This behavior was observed frequently in the visualization and accounts for the decreased height reached by bubble clusters interacting with case 2 vortices. This mechanism is similar to a scenario described by Sendstad and Moin.[13]

III. Recent Related Work

There has recently been an increase in research activity examining the structure of three-dimensional turbulent boundary layers. Some of this work corroborates our findings, whereas at least one study is in direct contrast.

Senstad and Moin[13] used direct numerical simulation to examine a fully developed channel flow turned by an impulsively applied spanwise pressure gradient. They found that the trajectory of fluid elements in the neighborhood of a vortex was changed by the crossflow so that the fluid ejected on the upflow side of a vortex originated farther from the wall in the three-dimensional turbulent boundary layer, creating a smaller shear stress. They also found that the vortices were convected in the spanwise direction relative to the low-speed streaks, and this tended to break up the streaks. A critical feature in both of these mechanisms is that the flow angle varies significantly with distance from the wall.

Flack and Johnston[14] studied two different flows: a rapidly turned boundary layer approaching a 45-deg swept step and a more slowly turned boundary layer on the endwall of a 30-deg bend. Both experiments were conducted at moderate Reynolds number ($Re_\theta = 1.5 \times 10^3$) in a large water channel facilitating flow visualization by dye injection and hydrogen bubbles. The streak spacing was observed to be approximately 100 wall units in agreement with two-dimensional turbulent boundary layer results. Ejections were visualized in the bend flow using a hydrogen bubble wire located around $y^+ = 3$ and showed asymmetry in the strength of ejections. However, case 2 vortices were seen to produce stronger ejections in contrast to our own results. A detailed mechanism involving multiple vortex interactions was hypothesized to explain the observed bubble motions. Although the precise mechanism was different from those of either Chiang and Eaton or Sendstad and Moin, the important similarity was that it again emphasized the importance of the mean gradient in the crossflow velocity.

Ha and Simpson[15] used multipoint hotwire and wall sensor measurements to examine the structure of a three-dimensional turbulent boundary layer forming ahead of a wing body junction at relatively high Reynolds number ($Re_\theta = 5.5 \times 10^3$). The streak spacing was found to be in the same range as observed in two-dimensional turbulent boundary layers. They used a 16-wire hotwire rake with the wires spaced logarithmically normal to the wall to measure the coherence function between velocity fluctuations near the wall and those above the wall. The coherence function is defined as

$$\gamma^2(f, \Delta y) = \frac{G_{12}^2}{G_{11} G_{22}}$$

where G_{11} is the velocity power spectrum at the near-wall probe, G_{22} is the velocity power spectrum measured at a probe Δy above, and G_{12} is the cross spectrum. Ha and Simpson defined the coherence length at a given frequency as the value of Δy where γ^2 has dropped to 0.27. The coherence length scale near the wall was found to decrease as three dimensionality increased. Ha and Simpson suggested a link with the observed reduction in the Reynolds shear stress. They also found that the coherent structures near the wall convected at an angle slightly different than the local mean velocity. They suggested that turbulent shear stresses may be pulling the coherent structures away from the direction of the local mean velocity. This conclusion is difficult to understand since the turbulent stresses are produced by the coherent structure. Fleming and Simpson[16] examined the same flow at a low Reynolds number ($Re_\theta = 5 \times 10^2$) in a water channel using a hydrogen bubble wire parallel to the wall. Qualitatively, they observed that the low-speed streaks appeared more stable in the three-dimensional flow as compared with the upstream two-dimensional turbulent boundary layer. Quantitative measurements indicated that the velocity difference between low- and high-speed streaks was smaller in the three-dimensional turbulent boundary layer.

IV. Summary and Discussion

The precise structural causes of shear-stress reduction in three-dimensional turbulent boundary layers appears to be just as elusive as the understanding of the basic structure in two-dimensional turbulent boundary layers. It seems likely that the near-wall structure is dependent on both the local pressure gradient field and on the boundary layer's history. It is probably not possible to define any characteristic of the near-wall structure in a three-dimensional boundary layer that would adequately characterize the wide range of flow geometries that produce mean flow three dimensionality. However, several common features have emerged from the experiments and simulation. First, the recent flow visualization experiments have shown that attached three-dimensional turbulent boundary layers contain the common features of other boundary layers, namely, low- and high-speed streaks and quasistreamwise vortices dominating the flow near the wall. Thus, it is appropriate to interpret the structure as a distorted version of the two-dimensional turbulent boundary-layer structure. Multipoint measurements and flow visualization both show that the crossflow produces asymmetry in the vortex structures with overall length scales being reduced and one sign of vortex generally weakened relative to the other. The most recent studies have pointed consistently to the variation in the flow direction across the inner region ($y^+ < 100$) as being a major factor in producing the structural distortion.

There are several implications of these findings. First, they show that the reduction of the shear stress by mean flow three dimensionality is not a disequilibrium effect. That is, three-dimensional boundary layers that persist for a long distance probably do not develop a new structure that reproduces two-dimensional turbulent boundary layer shear stress levels, as long as there is skewing across the near-wall region. Second, the structure will not be distorted if there is not significant skewing across the near-wall region that contains the quasistreamwise vortices. It is generally believed that the vortices scale on wall (viscous) variables so that increasing the Reynolds number would reduce their scale. There are only a few three-dimensional turbulent boundary layers studies in which the Reynolds number was varied over a significant range, but the present indication is that the height of the peak in the crossflow velocity profile scales on outer-layer variables. Therefore, as the Reynolds number increases, the vortices would get smaller relative to the size of the region of rapid skewing. We might expect that at very high Reynolds number the skewing across the height of the quasistreamwise vortices would be so small that the structure distortion would be negligible. A possible third implication is that shear stress might be reduced if asymmetry can be imposed on near-wall structures without imposing mean flow three dimensionality.

From the brief review presented here, it is apparent that the research community has focused on the near-wall region as the likely source of shear stress reductions. The hypothesis raised by Bradshaw and Pontikos[3] regarding the toppling of outer layer eddies has not received explicit attention. This mechanism is almost certainly active especially in flows where an initially two-dimensional turbulent boundary layer is skewed by a pressure gradient. It is not clear though how much effect such a mechanism might have on the overall flow development.

Acknowledgments

This work was supported by several grants from the Department of Energy, Office of Basic Energy Sciences, and NASA Ames Research Center. The work described here was done with my former students Shawn Anderson, Howard Littell, and Chisin Chiang and an academic visitor, Takaaki Shizawa.

References

[1]Johnston, J. P., and Flack, K. A., "Advances in Three-Dimensional Turbulent Boundary Layers with Emphasis on the Wall-Layer Regions," Dept. of Mechanical Engineering, Stanford Univ., Rept. MD-67, Stanford, CA, Feb. 1994.

[2]Abrahamson, S. D., and Eaton, J. K., "Heat Transfer Through a Pressure-Driven Three-Dimensional Boundary Layer," *Journal of Heat Transfer*, Vol. 113, No. 2, pp. 355–362.

[3]Bradshaw, P., and Pontikos, N. S., "Measurements in the Turbulent Boundary Layer on an 'Infinite' Swept Wing," *Journal of Fluid Mechanics*, Vol. 159, 1985, pp. 105–130.

[4]Anderson, S. D., and Eaton, J. K., "Reynolds Stress Development in Pressure-Driven Three-Dimensional Turbulent Boundary Layers," *Journal of Fluid Mechanics*, Vol. 202, 1989, pp. 263–294.

[5]Robinson, S. K., "Coherent Motions in the Turbulent Boundary Layer," *Annual Review of Fluid Mechanics*, Vol. 23, 1991, pp. 601–639.

[6]Shizawa, T., and Eaton, J. K., "Interaction of a Longitudinal Vortex with a Three-Dimensional Turbulent Boundary Layer," *AIAA Journal*, Vol. 30, No. 5, 1992, pp. 1180, 1181.

[7]Shizawa, T., and Eaton, J. K., "Turbulence Measurements for a Longitudinal Vortex Interacting with a Three-Dimensional Turbulent Boundary Layer," *AIAA Journal*, Vol. 30, No. 1, 1992, pp. 49–55.

[8]Pauley, W. R., and Eaton, J. K., "Experimental Study of the Development of Longitudinal Vortex Pairs Embedded in a Turbulent Boundary Layer," *AIAA Journal*, Vol. 26, No. 7, 1988, pp. 816–823.

[9]Littell, H. S., and Eaton, J. K., "An Experimental Investigation of the Three-Dimensional Boundary Layer on a Rotating Disk," Dept. of Mechanical Engineering, Stanford Univ., Rept. MD-60, Stanford, CA, 1991.

[10]Littell, H. S., and Eaton, J. K., "Turbulence Characteristics of the Boundary Layer on a Rotating Disk," *Journal of Fluid Mechanics*, Vol. 266, 1994, pp. 175–207.

[11]Senoo, Y., and Nishi, M., "Equilibrium Three-Dimensional Turbulent Boundary Layer on the End Wall of a Curved Channel," *Proceedings of the 2nd International JSME Symposium* (Tokyo), Sept. 1972, pp. 21–30.

[12]Chiang, C., and Eaton, J. K., "An Experimental Investigation of Corotating Disks and Single Disk Flow Structures," Dept. of Mechanical Engineering, Stanford Univ., Rept. MD-62, Stanford, CA, 1993.

[13]Sendstad, O., and Moin, P., "The Near-Wall Mechanics of Three-Dimensional Turbulent Boundary Layers," Dept. of Mechanical Engineering, Stanford Univ., Rept. TF-57, Stanford, CA, 1992.

[14]Flack, K. A., and Johnston, J. P., "Near-Wall Investigation of Three-Dimensional Turbulent Boundary Layers," Dept. of Mechanical Engineering, Stanford Univ., Rept. MD-63, Stanford, CA, 1993.

[15]Ha, S. M., and Simpson, R. L., "An Experimental Investigation of a Three-Dimensional Turbulent Boundary Layer Using Multiple-Sensor Probes," *Proceedings of the 9th Symposium Turb. Shear Flows* (Kyoto), Aug. 93, pp. 2-3-1–2-3-6.

[16]Fleming, J., and Simpson, R., "Experimental Investigation of the Near Wall Flow Structure of a Low Reynolds Number 3-D Turbulent Boundary Layer," AIAA Paper 94-0649, 1994.